

# Exploring Hot Pixel Characteristics for 7 to 1.3 micron Pixels

Glenn H. Chapman, Rohan Thomas, Klinsmann J. C. S. Meneses,  
Parham Purbakht,  
School of Engineering Science  
Simon Fraser University  
Burnaby, B.C., Canada, V5A 1S6  
[glennc@cs.sfu.ca](mailto:glennc@cs.sfu.ca), [rohant@sfu.ca](mailto:rohant@sfu.ca), [kcoelhos@sfu.ca](mailto:kcoelhos@sfu.ca),  
[ppourbak@sfu.ca](mailto:ppourbak@sfu.ca)

Israel Koren, Zahava Koren  
Dept. of Electrical and Computer Engineering  
University of Massachusetts  
Amherst, MA, 01003  
[koren,zkoren@ecs.umass.edu](mailto:koren,zkoren@ecs.umass.edu)

## Abstract

Digital imaging sensors “Hot Pixels” defects accumulate as the camera ages over time at a rate that is highly dependent on pixel size. Previously we developed an empirical formula that projects hot pixel defect growth rates in terms of defect density (defects/year/mm<sup>2</sup>). We found that hot pixel densities grow via a power law, with the inverse of the pixel size raised to the power of ~3, and almost the square root of the ISO (gain). This paper experimentally explores these defect rates as pixels approach the 2 to 1 micron size. We developed techniques for observing hot pixels both in regular DSLRs (7.5-4 $\mu$ m pixels) and in cell phones (1.3 $\mu$ m). Cell phones imagers have the smallest pixels, but require careful measurement to detect. First statistical analysis distinguishes potential defects from the nearby noise in a 5x5 pixel area around each pixel. Then linear regression fits the hot pixel equation to a sequence of dark field exposures from short (0.008 sec) to long (2 sec) and accepts only those with high statistical significance. This greatly improved the power law fit for the 2-1 micron pixels.

**Keywords-** imager defect detection, hot pixel development, APS defects rates, active pixel sensor APS, 7-1 micron pixels

## INTRODUCTION

Digital imaging sensors (cameras) like all integrated circuit devices, continuously develop defects over time. However, rather than the normal fabrication related degradation of other microelectronic devices, most in-field defects in digital sensors begin appearing soon after fabrication, are permanent in nature and their number increases continuously over the lifetime of the sensor. Yet imagers have the advantage in that the appearance of a defect, say a hot pixel, causes degradation in the circuit capability (image quality) rather than rendering the circuit useless as a single fault in a regular IC can do. Although the impact of imager defects can be overcome by recalibration and masking out the defect (i.e., interpolating the pixel from its neighboring pixel values), this can create a serious problem in many applications where image quality and pixel sensitivity are important.

Previously we have shown [1-6] that the most common type of defects that develop over time in digital imagers is “Hot Pixels”. This excludes fabrication time defects, which are mapped out in most digital cameras, but includes defects that develop as the camera ages. We have shown via statistical methods that hot pixels are most likely caused by cosmic ray damage [1-3], and therefore shielding or fabrication/design changes cannot fully prevent them from developing over time. The strength of hot pixels increases with exposure time, but the underlying parameters change little after formation (they are somewhat changed by the imager temperature). We have proposed an empirical formula, a power law relationship, which expresses the defect density  $D$  (defects per year per mm<sup>2</sup> of sensor area) as a function of the pixel size  $S$  (in microns) and sensor gain ( $ISO$ ). In this,  $D$  is proportional to the inverse of the

pixel size raised to about the third power (for APS or CMOS pixels), and to the square root of the gain. Hence, as pixel sizes decrease by a factor of 2, the defect density  $D$  grows by about 8 times, and with a doubling of  $ISO$ ,  $D$  increases by about 1.4 times.

This suggests that it is extremely important to study pixel sizes in the 2 to 1 micron range, which are seen in cell phones and many embedded devices. In previous papers we had obtained some data from the 2-1 micron pixels used in cell phones but from a very limited set of phones. In this paper we present new experimental, statistical and software techniques to extend our analysis to cell phones down to 1.2  $\mu$ m pixels. In particular, we now use the digital raw data available from cell phones combined with statistical confidence levels to gain higher accuracy in the cell phone hot pixel numbers. This is done to verify that cell phone pixels do not behave significantly different from the larger pixels, and therefore, a single power law formula can be used for all pixel sizes. Besides observing the number of hot pixels we also analyze the distribution of their parameters as a function of pixel size and sensitivity. With this analysis we gain an understanding of the growth model of defects, allowing us to determine where these new hot pixels are coming from as the pixel size gets smaller

## Hot Pixels

Our previous research has been gathered over 14 years of data [5,6], where we have performed manual calibrations on numerous commercial DSLRs, point and shoot cameras, and cell phone cameras. We used dark field exposures (i.e., no illumination) to identify defects, done at a range of exposure times (from 0.001 to 2 seconds) to test for stuck-high and partially stuck defects, and bright field exposures (i.e., uniform illumination at near saturation) to test for stuck-low defects. In all of these experiments we did not find any truly stuck defects. Instead, hot pixels were the dominating defect type.

Under dark field (no illumination), a regular pixel shows only a very low growth of signal with increasing exposure time – effectively only that of the background noise of the sensor. The dark response of both regular and hot pixels is demonstrated in Figure 1 showing the normalized pixel output versus exposure time (output level 0 represents no signal and 1 represents saturation). The dark response of a good pixel should be close to 0 (with some growth due to sensor noise) at any exposure time. By comparison, a classic hot pixel has a component that increases linearly with exposure time. In addition, we have found [5] that hot pixels can be categorized into two types: standard hot pixels, which have a component (dark current) that increases linearly with exposure time; and partially stuck or offset hot pixels, which have a term that can be observed even at no exposure.

The imaging sensor is often referred to as a digital system, but the actual pixel portion is an analog device. The classic assumed response of any pixel to illumination is given by equation (1), where  $I_{pix}$  is the response or output,  $R_{photo}$  is the incident illumination rate,  $R_{dark}$  is the dark current rate,  $T_e$  is the duration of the exposure,  $b$  is the dark current offset, and  $m$  is the amplification from the ISO setting.

$$I_{pix}(R_{photo}, R_{dark}, T_e, b) = m * (R_{photo} T_e + R_{dark} T_e + b) \quad (1)$$

For a good (regular) pixel, both dark current  $R_{dark}$  and offset  $b$  are, by design, as close to zero as the fabrication allows, so the output response gives a direct measure of the incident illumination. In a hot pixel,  $R_{dark}$  is significantly above the typical dark current noise level. This, combined with the offset  $b$ , create an additional signal that adds to the incident illumination, making the pixel output higher (i.e., brighter in pictures). With zero illumination or dark frame testing, the hot pixel offset model is shown in Equation (2).

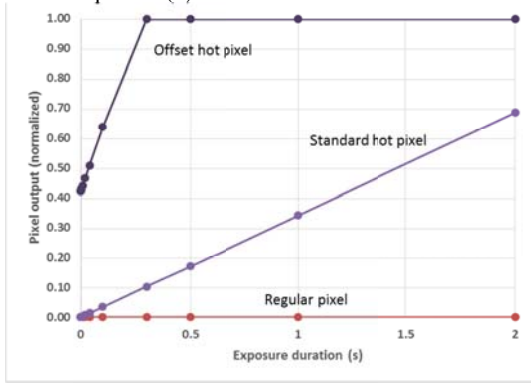


Figure 1: Comparing the dark response of imager pixels: a good regular pixel, a standard hot pixel, and an offset hot pixel.

$$I_{offset}(R_{dark}, T_e, b) = m * (R_{dark} T_e + b) \quad (2)$$

The dark response in Equation (2), sometimes called the combined dark offset, is nearly linear in  $T_e$ . The parameters  $R_{dark}$  and  $b$  are extracted in our experiments by fitting a linear curve to the pixel dark frame response versus the exposure time, as seen in Figure 1. For standard hot pixels, the offset  $b$  is zero. These hot pixels are most visible in longer exposures (in the order of one second) as they do not have an initial offset. However, in the partially stuck hot pixel case, the magnitude of the offset  $b$  affects the response and this defect will appear as a bright spot in all images. In our research, testing each camera involves typically 5 to 20 dark images at a wide range of exposure times from 0.001 to 2 seconds and ISOs from the lowest to the highest values in the camera. The data is taken in digital RAW formats to minimize the impact of software adjustments which distort the measured values, such as demosaicing of the color image, JPEG spreading of defects and color correction [10]). To minimize sensor temperature effects, a 30 second delay is placed after each dark field image. We have developed a Matlab analysis program [2-4] to identify the hot pixels in each camera, and extract the pixel parameters and locations.

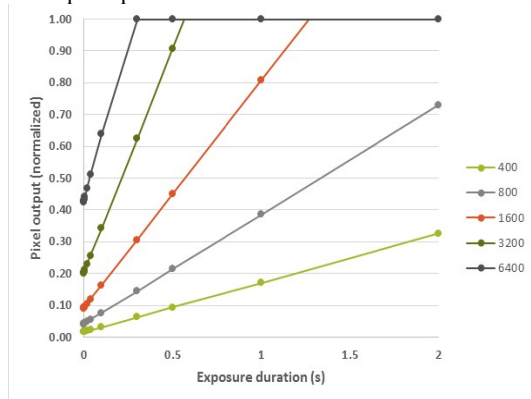


Figure 2: Dark response of one hot pixel at various ISO levels

The amplification of the pixel signal by the gain (ISO) setting also amplifies the values of both the hot pixel dark current  $R_{dark}$  and offset  $b$ . Figure 2 shows the measured values of the dark response for a typical hot pixel with increasing ISO levels. At low ISO, most defects have smaller values of  $R_{dark}$  and  $b$ , though significantly above the background noise levels at longer exposures. As the ISO amplification increases, both  $R_{dark}$  and  $b$  increase dramatically, scaling linearly with the ISO (see Equation (1)). At ISO 12800, the dynamic range of the pixel is reduced by 40% solely due to the offset  $b$ , and at ISO 25600 the pixel is near saturation at all exposures. The significant number of hot pixels with offsets has previously suggested to us that what seem to be stuck-high pixels, may actually be hot pixels with very high offsets

## Defect Growth Rate

We have shown that hot pixel defects occurrences are randomly spaced across the imager [1-6]. Statistical analysis indicated that they are created by a random source such as cosmic rays [10]. The literature shows that other authors have reached a similar conclusion, and have argued that neutrons seem to create the same hot pixel defect types [7,8]. Using linear regression curve fitting to all our camera data over all ISOs we developed in [9,11] an empirical formula to relate the defect density  $D$  (defects per year per  $\text{mm}^2$  of sensor area) to the pixel size  $S$  (in microns) and sensor gain (ISO) via the following equations:

For APS pixels:

$$D = 10^{-1.12} S^{-3.15} \text{ISO}^{0.525} \quad (3)$$

For CCD sensors

$$D = 10^{-1.849} S^{-2.25} \text{ISO}^{0.687} \quad (4)$$

Figure 5 shows a plot of Equation (3) for the full test range. These equations indicate that the defect density increases drastically when the pixel size falls below 2 microns (see Figure 6), and is projected to reach 12.5 defects/year/ $\text{mm}^2$  at ISO 25,600 (which is already available on some high-end cameras).

Since the current trend is to further reduce the size of pixels, these experimental results project that the number of these defects will increase to high levels, emphasizing the need to understand how the development rate of these defects increases as the pixel size reduces.

## Cell Phone Hot Pixel Detection

Cell phones generally have the smallest pixels in general commercial uses, due to the desire by companies to offer the highest number of megapixels in a small camera at a very low cost. Generally, the price of the camera system in a cell phone is ~\$10, compared to DSLRs where the price is \$300-\$5000. As a result, current cell phone pixels are in the 1.34 to 1.2  $\mu\text{m}$  range, and imager areas in the 24  $\text{mm}^2$  range.

This drive for smaller pixels unfortunately results in some significant problems in detecting hot pixels in the cell phone imagers. First, only the most recent operating systems, Android 7.0 or greater, allow a digital raw output, and not all camera apps support this. Second, digital raw is not the standard output for these cameras, hence it has much higher noise levels than DSLRs where considerable noise suppression effort is made in both pixel design, and by software applied before the digital raw output. This results in two significant limitations on phone images. First, maximum output sensitivity is relatively low at 800 ISO, compared to the >6400 ISO in 2017 DSLRs. Second, the maximum exposure time for current cell imagers before noise becomes too high is ~2 sec., compared to >30 sec. for DSLRs. Another complicating factor is that cell phones have

many other processes executing, hence controlling device temperature is important. By comparison, in DSLRs the processor is idle between pictures so it is possible to space out the photos in time to remove the heat generated by taking an image.

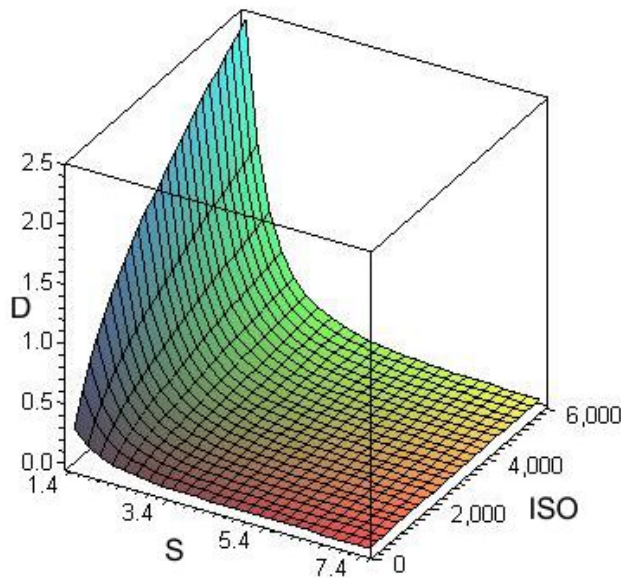


Figure 5: Fitted power law for APS: defect density ( $D$ =defects/year/ $\text{mm}^2$ ) vs. pixel size  $S$  ( $\mu\text{m}$ ) and ISO ( $I$ )

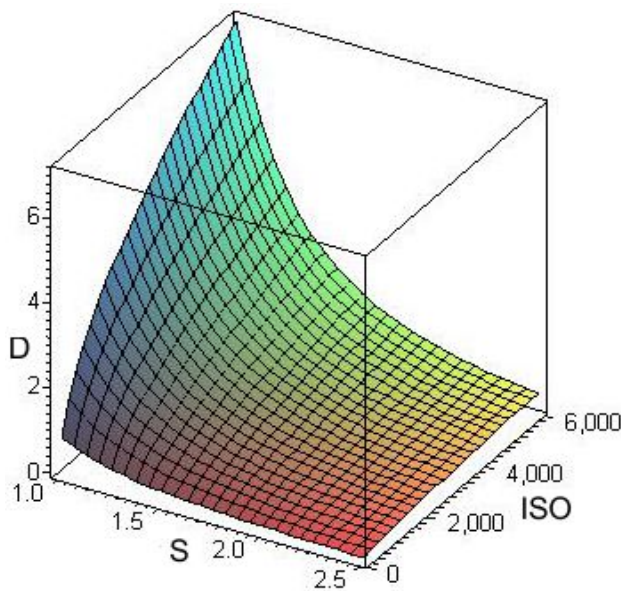


Figure 5: Fitted power law for APS in the 1 to 2.5  $\mu\text{m}$  pixel range: defect density ( $D$ =defects/year/ $\text{mm}^2$ ) vs. pixel size  $S$  ( $\mu\text{m}$ ) and ISO ( $I$ )

After many experiments we developed an effective methodology for testing the cell imagers. First, to keep the phones cool we put them into airplane mode (i.e., turned off the communications which generate considerable heat). Then, we placed the phones in a refrigerator (at  $\sim 4^\circ\text{C}$ ) on the metal frame to maximize cooling. This reduces the phone temperature by about  $16^\circ\text{C}$ , resulting in considerable noise reduction. For dark

images both the imager lens and the phone display were covered to allow totally dark images. Triggering the phone camera was done remotely via USB connection from an external computer using the Vysor app on the cell phone.

We then checked the noise histogram of the raw files both at the beginning and end of tests to confirm that there is no increase in temperature driven noise during the experiment. Figure 6 is the noise plot of a dark field image for one cell, which shows a 2 second exposure at 800 ISO pixel histogram showing a 99% noise point of about 43 or 17% of the max 255 value. This noise level is much higher than in DSLRs where at 6400 ISO in dark frames typical pixel counts give the 99% percentile of noise as usually  $<10\%$ .

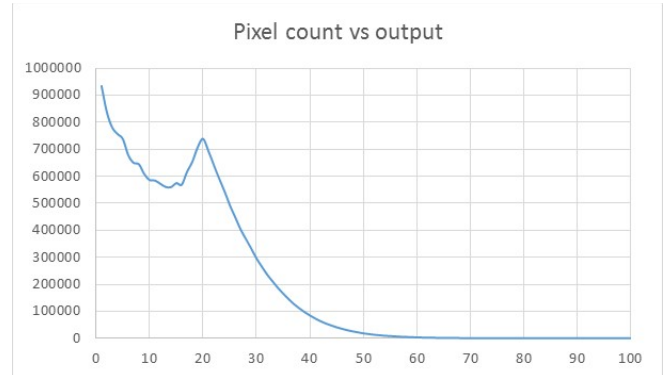


Figure 6: Cell phone dark image pixel count vs output (0 to 255) at 800ISO

As noted before, the cell phone data is noisy so a simple threshold type analysis such as that often used in DSLRs will not work. As with the DSLRs we took a range of exposure times from 0.008 sec to 2 sec (the longest reasonable on cell phones). We also repeated each exposure 3 to 10 times and did a statistical average of the value at each pixel for each exposure time as part of our analysis. Then we created a Matlab program that searched first for any pixels where the long exposures were above the threshold. We then did least squares regression fit for the hot pixel equation (2), which included calculating the standard deviation SD of the dark current  $R_{dark}$  and offset  $b$  estimated values. Unless the statistical Student  $T$ -ratio (i.e., ratio of the fitted coefficient to the SD) exceeded 3 for the dark current and/or the offset, the pixel was not considered a hot pixel. Indeed offsets  $b$  that meet this  $T$ -ratio were seen in the shortest exposures (0.008 sec.). This combination of multiple measurements and statistical significance is much more rigorous than used in the DSLR tests. Three cell phone cameras were used in the current test, all with a pixel size of  $1.34 \mu\text{m}$ .

### Nearest Noise Criterion Hot Pixel Detection

DSLRs employ noise reduction algorithms which suppress the background noise and these tend to make use of the local noise information. To enhance detection we are now adding a new procedure we call the Nearest Noise Criterion detection to replace the single threshold initial detection test. Since dark field noise varies strongly about the imager it is much better to compare a potential hot pixel to the local noise of the surrounding pixels. Again we take the same 3 or more dark field images and consider the longer exposures (0.033sec or longer). We take the  $5 \times 5$  pixel square around each pixel being tested (see Fig. 7) and gather noise statistics on the 24 near pixels for all 3 images ( $I_{i,j}(k)$  values where  $i = j \neq 0, k=1..3$ ), plus values of the central hot pixel suspect  $I_{0,0}$  for all  $k$ . We measure the mean  $I_{nearm}$  and standard deviation ( $\sigma$  or SD) of these neighboring 24 pixels for the 3 images ie 72 data points. Values were gathered as 16 bit (i.e. 65,536 max). Then we reject any case where:

any of the 3 central pixel values are within  $3\sigma$  of the noise mean

$$I_{0,0}(k) > (I_{\text{nearm}} + 3\sigma) \text{ for all } k = 1..3 \quad (5)$$

or when any central pixel is less than the highest surrounding pixels.

$$I_{0,0}(k) > I_{i,j}(k) \text{ for } i=j \neq 0, k=1..3 \quad (6)$$

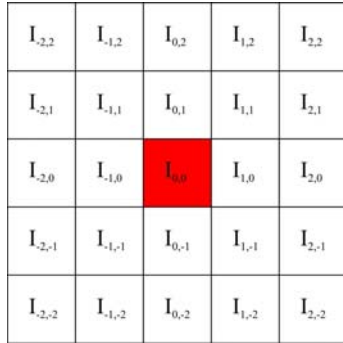


Figure 7: 5x5 square of near neighbors of the hot pixel  $I_{0,0}$

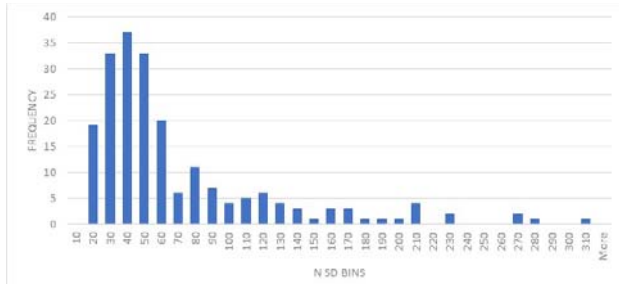


Figure 8: Distribution of separation of mean hot pixel  $I_{0,0}$  to near neighbors noise mean in standard deviation  $\sigma$  units

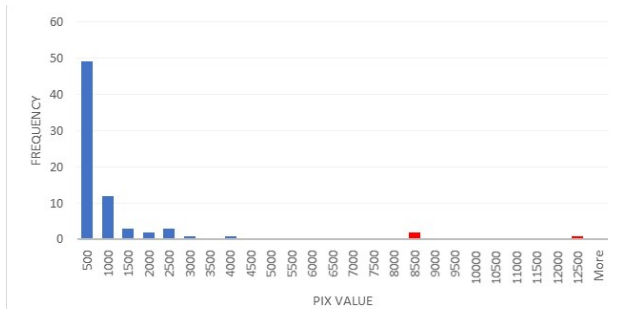


Figure 9: Near neighbor noise distribution (blue) and hot pixel  $I_{0,0}$  (red) of typical minimum pixel ( $12.8\sigma$ ) separation,  $\sigma = 745: 0.033$  sec exposures

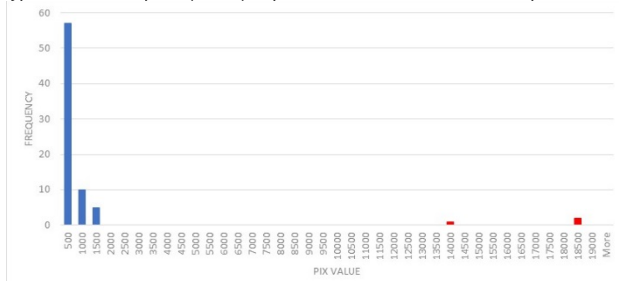


Figure 10: Near neighbor noise distribution (blue) and hot pixel  $I_{0,0}$  (red) of typical median pixel ( $45.2\sigma$ ) separation:  $\sigma = 369: 0.033$  sec exposures

This additional criterion is applied to identify candidate hot pixels instead of the simple threshold described previously (applied for the 0.033 or longer exposures). Then again, as described in the previous section, we applied the least squares

regression fit over the whole exposure range, to show that the suspected hot pixel had dark current  $R_{\text{dark}}$  or offset  $b$  at sufficient statistical significance. Using this combination of tests Fig. 8 shows for the hot pixels the resulting number of SDs separation between the mean  $I_{\text{nearm}}$  of near neighbors and the hot pixel  $I_{0,0}$  for the 3 exposures of the same duration. For the “A” cell phone with 208 hot pixels under these criterion this had a minimum separation from near neighbor noise mean  $I_{\text{nearm}}$  was  $10.3\sigma$  and while the average separation of was  $45\sigma$ , all showing very high statistical significance. Fig. 9 shows the noise and hot pixel distribution of typical minimum pixel ( $12.8\sigma$ ) and Fig 10 for a typical median separation pixel ( $45.2\sigma$ ).

## Hot Pixel Parameters & Defect Growth Rate

In previously reported research [5] we have shown that the size of the hot pixel defect is very small, less than 5% of the pixel 7 micron size. Current results confirm this – there is no indication that a hot pixel damage extends beyond the pixel boundary, even with the smallest (1.34 microns) pixels of the cell phone. Otherwise we would see adjacent hot pixels due to the spread of the damage.

By assuming that the damaged point that creates the hot pixel is independent of the actual size of the pixel, we would expect that as the pixel shrinks, the defect rate would scale with the reduction in the pixel area,  $S^2$ . Still, our current formula (Equation 3) suggests that a shrinkage of the pixel size by a factor of 2 results in an 8.9 times increase in the defect rate, which is the pixel size to about the third power. Higher imager sensitivities (ISOs) increase this effect by the square root of the increase in ISO. It is important to extend this to the smallest pixel sizes, 2-1 micron range. But we must ask the question – considering the significant changes in the pixel designs between the 7 micron devices down to the cell phone pixels (1.34  $\mu\text{m}$ ) can a single formula cover all the pixels? However if it does not we should have seen significantly higher errors in the fit (i.e. residuals) or a sudden change in the error for the smaller pixels, which do not.

Let us compare the hot pixel defect density rate  $D$  distributions of two DSLR cameras types with 6.3  $\mu\text{m}$  and 4.3  $\mu\text{m}$  pixels over ISOs from 400 to 6400 values (these cameras are respectively 6 and 5 years old). These cameras have sensor areas in the 342 sq. mm size.

Table 1: Defect Density  $D$  (Defects/ $\text{mm}^2/\text{year}$ ) for various ISO values at pixel sizes  $S = 6.3\mu\text{m}$  and  $4.3\mu\text{m}$  (average data)

ISO	S=6.3 $\mu\text{m}$	S=4.3 $\mu\text{m}$
400	0.011	0.012
800	0.015	0.014
1600	0.017	0.036
3200	0.021	0.109
6400	0.026	0.249

Table 2: Cell Phone Defect Density  $D$  (Defects/ $\text{mm}^2/\text{year}$ ),  $S = 1.34\mu\text{m}$ , ISO 800

Cell	D	T-Stat
A	0.875	6.2
B	0.417	12.5
C	0.463	12.1

In Table 2 we show the effective density  $D$  for hot pixels in 3 cell phones, with a pixel size of 1.34  $\mu\text{m}$ , sensor area of 24  $\text{mm}^2$  and ISO of 800. Using the regression fit method described previously it was found that the statistical significance of the dark current in these hot pixels is very high, with a Student T-ratio (dark current parameter divided by the standard deviation of that parameter) of between 4.7 and 36, and an average of 10, way higher confidence than the 95% significance level of 3.

This result shows that now that RAW data files are fully supported in certain cell phones, it is possible to obtain reliable hot pixel defect rates for these small pixels. Note how the D rate is for the cell phone data of Table 2 averages nearly 40 times higher compared to that at 800 ISO in the averaged DSLR defect rates (among several cameras) of Table 1.

With these new results we have now been able to significantly improve the power law fit results. Using additional data from new tests of the DSLRs and replacing our previous less reliable cell phone data (gathered without cell phone RAW output files). We now see an increase in D for APS pixels of

$$D=10^{-1.16}S^{-3.03}ISO^{0.506} \quad (7)$$

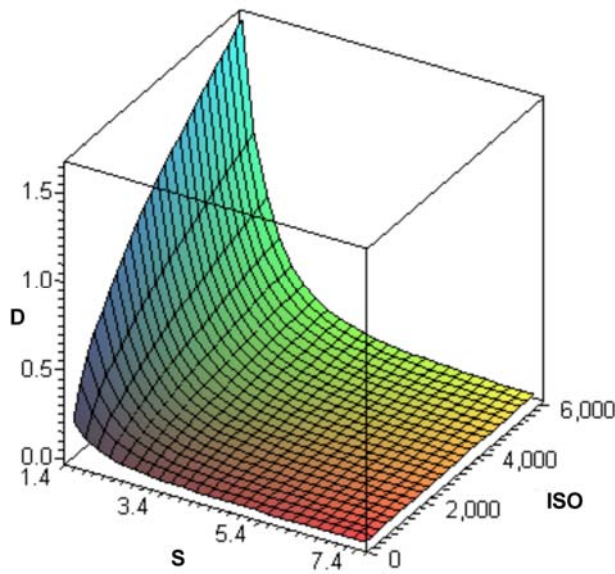


Figure 11: Fitted power law for APS: defect density ( $D$ =defects/year/ $mm^2$ ) vs. pixel size  $S$  ( $\mu m$ ) and ISO ( $I$ ) including the cell phone hot pixel data

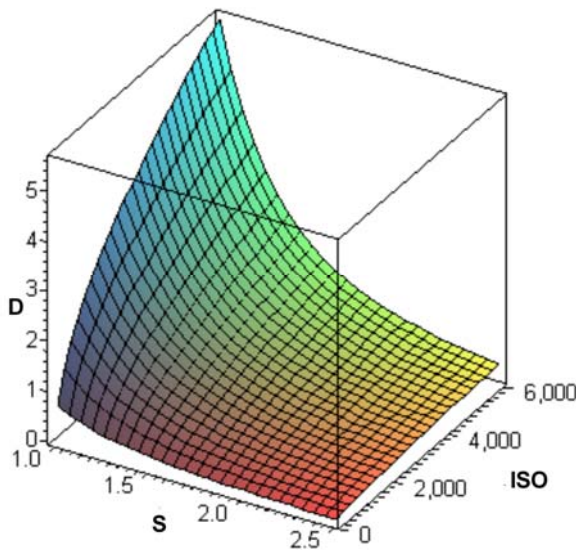


Figure 12: Fitted power law for APS in the 1 to 2.5  $\mu m$  pixel range: defect density ( $D$ =defects/year/ $mm^2$ ) vs. pixel size  $S$  ( $\mu m$ ) and ISO ( $I$ ) including the cell phone hot pixel data

Figure 11 shows the resulting plotted curves for the full size range while Figure 12 shows in higher resolution the details of

the behavior in the 1 to 2.5 micron range. Note especially that the pixel size power has decreased to 3.03, from the previous 3.15. However this is still within the standard deviation of the dark current fit parameter which is 0.15 so the change is within that expected statistically. Actually the new hot pixel statistical selection methodology gives D rates which are a much better fit in terms of the fit residuals (difference between the fitted projections and the actual measured D rates) than our older threshold method of detecting cell phone hot pixels. The ISO power has also decreased to 0.506 from 0.525, again within the SD of 0.095 for this parameter. Hence there is nondication that there is a sudden change in the defect rates D in spite of the significant changes in the pixel designs.

If this empirical formula continues to hold true the implications are that as pixel size  $S$  shrinks towards zero the defect density rate increase towards infinity. That suggests cosmic ray generated defects might be a significant limit in how small pixels can useful be shrunk.

## Conclusions

In this paper, we have developed a reliable method of measuring hot defect rates in the small (1.34  $\mu m$  pixel) cell phone imagers due to the RAW file data now being available. The key is using enhanced statistical methods to account for the much higher noise level in these small pixels with only the simplest of RAW data output. With this we have significantly enhanced the accuracy of the power law fits at the small (2- $\mu m$ ) pixel region beyond that of previous results. With many new cell phones having RAW file output can rapidly gain more data on small pixels.

The empirical formula predicting growth in the defect density rate shows only small parameters changes, within the previous error limits, suggesting that it continues to hold down to the 1 micron pixel size. Its implications for limits on shrinking pixel designs are worth considering.

## References

- [1] J. Dudas, L.M. Wu, C. Jung, G.H. Chapman, Z. Koren, and I. Koren, "Identification of in-field defect development in digital image sensors," *Proc. Electronic Imaging, Digital Photography III*, v6502, 65020Y1-0Y12, San Jose, Jan 2007.
- [2] J. Leung, G.H. Chapman, I. Koren, and Z. Koren, "Statistical Identification and Analysis of Defect Development in Digital Imagers," *Proc. SPIE Electronic Imaging, Digital Photography V*, v7250, 742903-1 - 03-12, San Jose, Jan 2009.
- [3] J. Leung, G. Chapman, I. Koren, and Z. Koren, "Automatic Detection of In-field Defect Growth in Image Sensors," *Proc. of the 2008 IEEE Intern. Symposium on Defect and Fault Tolerance in VLSI Systems*, 220-228, Boston, MA, Oct. 2008.
- [4] J. Leung, G. H. Chapman, I. Koren, Z. Koren, "Tradeoffs in imager design with respect to pixel defect rates," *Proc. of the 2010 Intern. Symposium on Defect and Fault Tolerance in VLSI*, 231-239., Kyoto, Japan, Oct 2010.
- [5] J. Leung, J. Dudas, G. H. Chapman, I. Koren, Z. Koren, "Quantitative Analysis of In-Field Defects in Image Sensor Arrays," *Proc. 2007 Intern. Sym on Defect and Fault Tolerance in VLSI*, 526-534, Rome, Italy, Sept 2007.
- [6] J. Leung, G.H. Chapman, Y.H. Choi, R. Thomson, I. Koren, and Z. Koren, "Tradeoffs in imager design parameters for sensor reliability," *Proc., Electronic Imaging, Sensors, Cameras, and Systems for Industrial/Scientific Applications XI*, v 7875, 7875011-0112, San Jose, Jan. 2011.
- [7] A.J.P. Theuwissen, "Influence of terrestrial cosmic rays on the reliability of CCD image sensors. Part 1: experiments at room

temperature,” *IEEE Transactions on Electron Devices*, Vol. 54 (12), 3260-6, 2007.

- [8] A.J.P. Theuwissen, “Influence of terrestrial cosmic rays on the reliability of CCD image sensors. Part 2: experiments at elevated temperature,” *IEEE Transactions on Electron Devices*, Vol. 55 (9), 2324-8, 2008.
- [9] G.H. Chapman, R. Thomas, I. Koren, and Z. Koren, “Empirical formula for rates of hot pixel defects based on pixel size, sensor area and ISO”, *Proc. Electronic Imaging, Sensors, Cameras, and Systems for Industrial/Scientific Applications XIII*, v8659, 86590C-1-C-11 San Francisco, Jan. 2013.
- [10] J. Leung, “Measurement and Analysis of Defect Development in Digital Imagers, MSc thesis, Simon Fraser University, School of Engineering Science, Burnaby, BC Canada, 2011.
- [11] G.H. Chapman, R. Thomas, I. Koren, and Z. Koren, “Hot Pixel Rate Behavior as Pixel Sizes go to 1 micron”, *Proc. Electronic Imaging: Image Sensors and Imaging Systems 2017*, pp 39-45, San Francisco Feb. 2017.

### **Author Biographies**

Glenn Chapman, Professor and Chair, School of Engineering Science, Simon Fraser University, Canada, researching in defects in digital image sensors. BSc and MSc Physics Queen’s University, and PhD McMaster University, Canada.

Israel Koren, Professor, Electrical and Computer Engineering at the University of Massachusetts, Amherst and a fellow of the IEEE. BSc, MSc and DSc Technion - Israel Institute of Technology.

Zahava Koren, senior researcher, University of Massachusetts, Amherst. B.A and M.A degrees in Mathematics and Statistics, Hebrew University, Jerusalem, and D.Sc. degree in Operations Research, Technion - Israel Institute of Technology.